SciMedCentral

JSM Chemistry

Research Article

Structure-based Design and Pharmacological Study of Fluorinated Fused Quinazolines as Adenosine A_{2B} Receptor Antagonists

Balakumar Chandrasekaran, Pran Kishore Deb, and Raghuram Rao Akkinepalli*

Pharmaceutical Chemistry Division, Panjab University, India

***Corresponding author**

Raghuram Rao Akkinepalli, Pharmaceutical Chemistry Division, Kakatiya University, Warangal, Andhra Pradesh - 506 009, India, Tel: 91-870-2446259; Fax: 91-870-2543508; Email: raghumed@kakatiya.ac.in

Submitted: 23 Febraury 2017

Accepted: 12 May 2017

Published: 15 May 2017

ISSN: 2333-6633

Copyright

© 2017 Akkinepalli et al.

OPEN ACCESS

Keywords

- AR antagonists
- Fused quinazolines
- Molecular docking
- Accelrys
- GOLD
- GLIDE

Abstract

Novel fluorinated fused quinazolines with varying substitution pattern were designed based on bioisosteric replacement of active groups of the known adenosine A_{2B} receptor (A_{2B} AR) antagonists. Further, physico-chemical properties were computed for the newly designed ligands. The designed ligands were evaluated by three different commercially available molecular docking (*in silico*) software tools against A_{2B} AR structure as suitable target protein. Molecular docking investigation of the designed ligands onto the active-site of A_{2B} AR indicated higher docking scores and favourable molecular interactions. Based on *in silico* results, selected compounds were evaluated for *in vitro* adenylyl cyclase activity against hA_{2B} AR.

INTRODUCTION

Adenosine receptors (ARs) belong to the super family of G protein-coupled receptors (GPCRs), having four core subtypes (A_1, A_{2A}, A_{2B}, and A_3) all of which exhibit distinct physiological functions [1]. A_1 ARs are present in the brain with major allocation and minimum levels in the heart, kidney, adipose tissue, stomach, spleen and liver [2]. A_{2A} ARs are highly distributed in the blood platelets, striatum, nucleus accumbens and olfactory tubercle [3], while A_{2B} ARs regulates a number of physiological and pathological events that involve lungs, blood vessels and bladder [4]. A_3 ARs are highly expressed in immune cells, lung and liver and at lower densities in heart, aorta and brain [5]. Both agonists and antagonists of all AR subtypes are useful as therapeutic agents in treating a variety of diseases. In particular, A_{2B} AR is the least characterized among the ARs primarily due to the lack of appropriate and precise ligands. Selective A_{2B} AR antagonists were shown to decrease inflammatory conditions and were found to be promising candidates for the treatment of asthma and diabetes [6,7]. Some of the selective A_{2B} AR antagonists reported with anticancer properties and also as agents to treat various pathological events associated with cardiovascular diseases [8-10]. During the past decade, a number of potent and selective ARs antagonists have been developed, including both xanthines and non-xanthine derivatives. Some of the ARs antagonistic compounds entered clinical trials too [11] and some of the potent molecules are presented in Figure 1.

Quinazoline is one of the interesting pharmacologically active scaffolds reported to exhibit diverse biological activities [12,13]. CMB-6446, a quinazoline analogue reported as potent hA_{2B} AR antagonist with a binding K_i value of 112 nM [14]. In some of the reported ARs antagonists, fluoro or trifluoromethyl substituents on active scaffolds showed a profound synergistic effect on the physical and /or biological properties [15].

Computational tools such as *in silico* molecular docking is one of the well known molecular modeling techniques widely employed in drug design and discovery. It serves as a reliable tool to identify novel therapeutic agent for various targets and thus resulting in the establishment of ligand-target interactions. Moreover, *in silico* data can guide the drug design strategies to optimize the structure [16] thereby obtaining more potent compounds. Hence, in continuation of our efforts [17-19] in obtaining novel fluorinated quinazolines as human A_{2B} AR antagonists, we herein designed and investigated the application of structure-based molecular docking with *in vitro* validation by adenylyl cyclase activity assay Figure 1.

MATERIALS AND METHODS

Design of fluorinated heterofused-quinazolines as ARs antagonists

New fluorinated heterofused-quinazolines (ARR/PL-1 to 14) were designed based on bioisosteric replacement of known A_{2B} AR antagonist (CMB 6446) [14]. Global physicochemical properties, steric and molecular surface descriptors of an AR

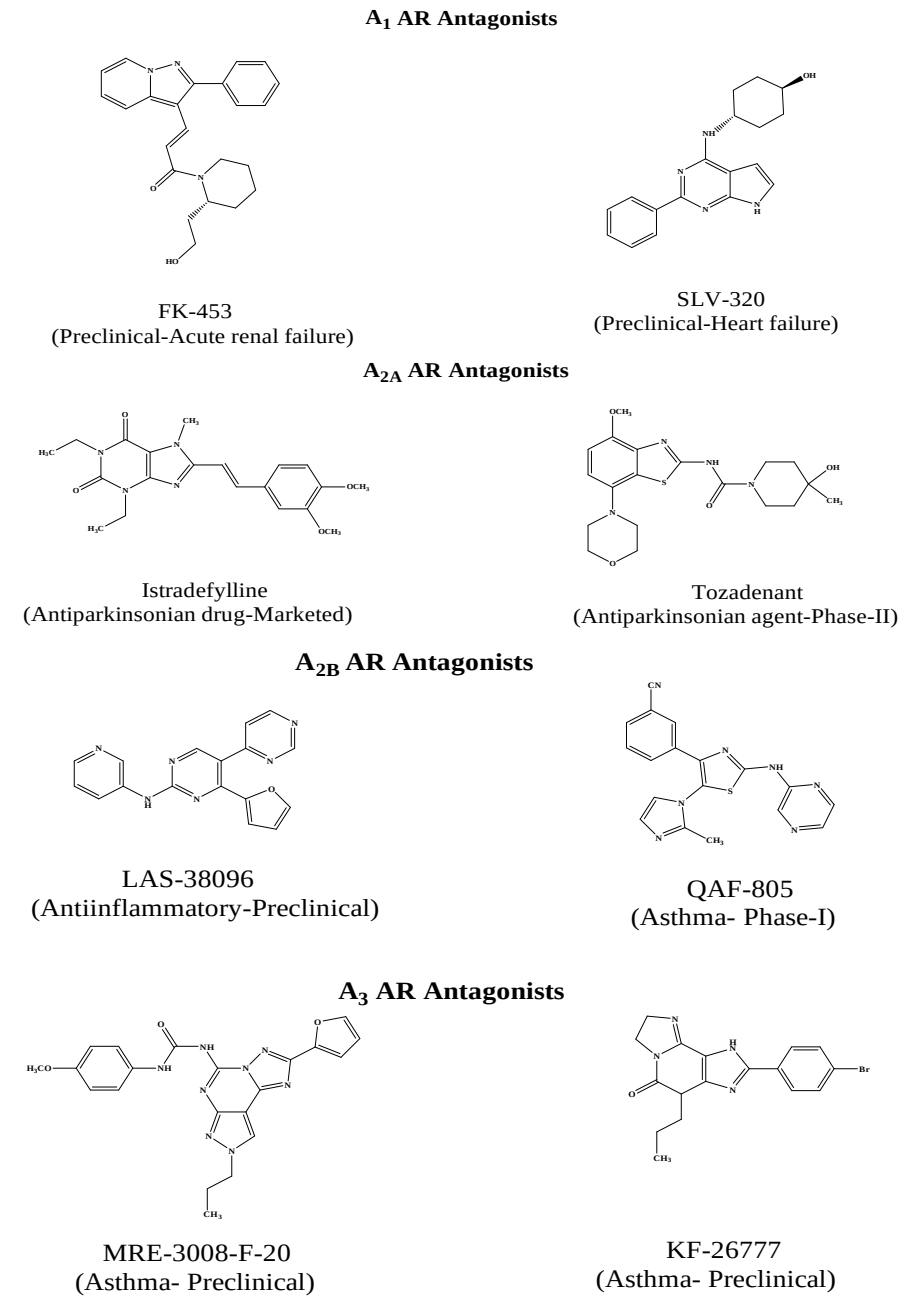

Figure 1 Potent ARs antagonists reported in literature.

antagonist (Figure 2, CMB 6446) and the designed fluorinated quinazoline-based ligands Figure 3 were computed.

Percentage similarity

Based on these properties, the percentage similarity [20] of the respective molecule was computed by using the formula:

Similarity (%) = (1-R) x 100

R= $\sqrt{d_i^2}$ is quadratic mean (also known as the root mean square) and is a measure of central tendency. Where distance d_i of a particular target compound "i" to CMB 6446 could be presented according to the formula:

$$d_i^2 = \sum_{j=1}^{n}(1-X_{i,j}/X_{i,let})^2/n$$

Where $X_{i,j}$ is value of molecular parameters i for compound j; $X_{i',let}$ is the value of the same molecular parameter i for CMB 6446; n is the total number of the considered molecular parameters.

Molecular docking

Homology model of A_{2B} AR was employed as a protein target. Different docking programmes [LigandFit module of Accelrys (Discovery Studio 2.1 version) [21], Glide module of Schrodinger

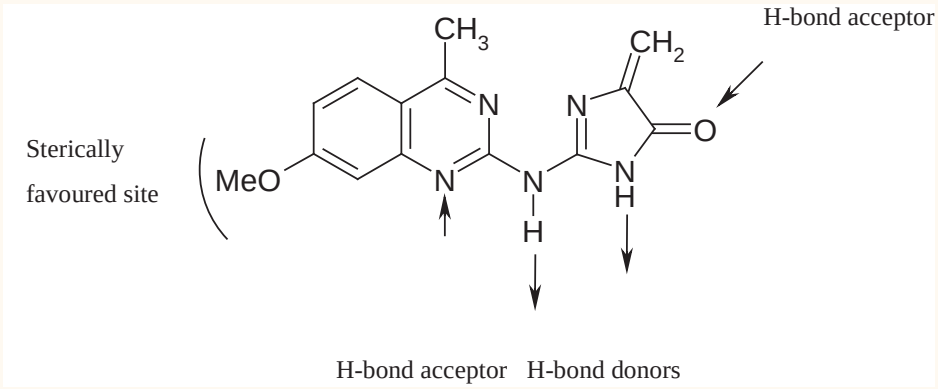

Figure 2 CMB 6446.

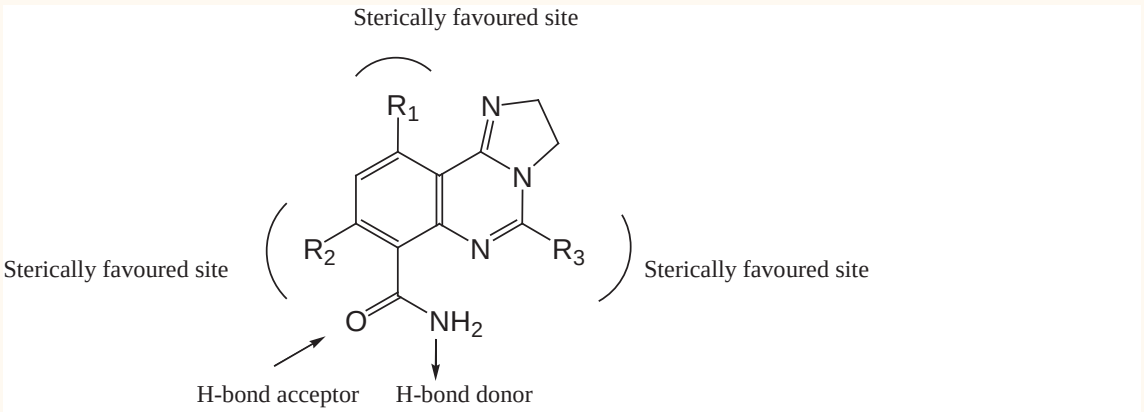

R_1 = R_2 = -CF_3, -C_6H_5; R_3= Furyl, 4-hydroxyphenyl, thienyl, 2-chlorofuryl, 2- chloropyryl, 2-cyano-3,4-dimethylpyryl, 3-methylthienyl

Figure 3 The designed series of fluorinated quinazolines (ARR/PL-1 to 14).

(Maestro 9.1 version) [22] and GOLD (CCDC, 4.0.1 version) [23] were employed for the preparation of the protein, ligand and the docking run. Molecular modeling was performed using Dell Precision work station T3400 running Intel Core2 Duo Processor, 4GB RAM, 250 GB hard disk, and NVidia Quadro FX 4500 graphics card. Molecular docking can be described as two components: a search strategy and an evaluation of docking results (scoring function). The search algorithm generates optimum number of poses including experimentally determined binding mode. The docked poses were scored using different scoring functions (Goldscore (GS), G-score, IFD Glide score and Dock score) to find the better docking pose.

Homology model of A_{2B} adenosine receptor (A_{2B} AR)

Like most other transmembrane GPCRs, the high-resolution A_{2B} AR crystal structure has not been solved to date, thus only homology model can be used to perform docking studies. In our studies, we employed homology model of A_{2B} AR generated by Swiss-model (automated protein structure homology-modeling) server [24a,b] accessible via the ExPASy web server, or from the program Deep View (Swiss PDB-Viewer). The model utilized the crystal structure of A_{2A} AR as an appropriate template.

PREPARATION OF PROTEIN, LIGAND STRUCTURES AND DOCKING RUN - LIGANDFIT

Preparation of protein

All hydrogen atoms were included to the protein which was subjected to minimization using steepest descent (gradient <0.1) and conjugate gradient algorithms (gradient <0.01) using the CHARMm force field [25]. The defined receptor was generated, different binding sites were identified based on the presence of cavities and appropriate active-site was selected within a 10 Å radius from the center of the bound ligand / active-site amino acid residue (if required, partitioned up to 5 levels). Stochastic conformational searching was applied to the ligands with a number higher than the default number of Monte Carlo search steps to ensure extensive conformational sampling.

Prepared protein was defined as receptor and any bound ligands were excluded from the calculations before a docking run. Active-site was defined around 10 Å from the bound ligand / active-site residue.

Preparation of ligands

'Prepare Ligands' module was used for preparation of ligands

for docking run. It is a utility of Accelrys Discovery Studio 2.1 software that combines tools for generating 3D structures from 1D (Smiles) and 2D (SDF) representation, searching for tautomers and steric isomers and performs a geometry minimization for ligands. The ligands were minimized by CHARMm force field with default setting.

Docking run

LigandFit (a shape-based method) employs a cavity detection algorithm. A shape comparison filter is combined with Monte-Carlo techniques to generate ligand conformations and dock them into the active-site of a protein. Docking was performed with Monte Carlo simulations using the CHARMm force field. A grid resolution was set to 0.5 Å (default) and the ligand-accessible grid was defined such that the minimum distance between a grid point and the protein is 2.0 Å (hydrogen atoms) and 2.5 Å (heavy atoms). The grid extends from the defined active-site to a distance of 5 Å in all directions.

The top 10 conformations were saved after rigid body minimizations of 1000 steps for analysis of docking poses. Dockscore, Ligscore1 and Ligscore2, PLP1, PLP2, JAIN, PMF and Dock scores were determined. Energy minimized conformer with best Dock scores were considered for the identification of interacting amino acid residues with ligands. Binding orientation and various interactions (H-bond, hydrophobic and vdW interactions) were also determined.

Preparation of protein, ligand structures and docking run - GLIDE (Grid based ligand docking with energetics)

Preparation of protein: The multistep Schrodinger's protein preparation wizard tool (PPrep) has been used for protein preparation. The molecular (homology) model of A_{2B} AR was taken and refined. Hydrogens were added to protein via the Maestro interface leaving no lone pair and using an explicit all atom model. Protein preparation performs the following steps: assigning of bond orders, addition of hydrogen atoms, and optimization of hydrogen bonds by flipping amino side chains, correction of charges, and minimization of the protein complex. The tool neutralized the side chains that are not close to the binding cavity and do not participate in salt bridges. This step is then followed by restrained minimization, which reorients side chain hydroxyl groups and alleviates potential steric clashes. The complex obtained was minimized using OPLS_2005 force field [26] with Polack-Ribiere Conjugate Gradient (PRCG) algorithm. The minimization was terminated either completion of 5,000 steps (or) after the energy gradient converged below 0.05 kcal/mol.

Preparation of ligands: Structures of the ligands were sketched using built panel of Maestro and taken in .mae format. LigPrep module was used for ligand preparation. LigPrep is a utility of Schrodinger software suit that combines tools for generating 3D structures from 1D (Smiles) and 2D (SDF) representation, searching for tautomers and steric isomers and perform a geometry minimization of ligands. The ligands were minimized using OPLS-2005 force fields with default setting.

Receptor-Grid generation and docking: Glide, extra precision (XP) mode used for docking protocol. The best 10 poses and corresponding scores have been evaluated using Glide in standard precision (SP) mode for each ligand. For each screened ligand, the pose with the lowest Glide SP score has been taken as the input for the Glide calculation in XP mode. To soften the potential for non-polar parts of the receptor scaled van der Waals radii of receptor atoms defined as 1.00 with partial atomic charge 0.25. G-score and six docking descriptors were calculated for each of the best docked pose.

GOLD (Genetic Optimization for Ligand Docking)

GOLD is a ligand-docking application that utilizes a genetic algorithm (GA) to explore ligand conformation flexibility and orientation with partial flexibility of the protein, and satisfy ligand-binding requirements. One advantage of GOLD over many other docking algorithms is that it allows for both unconstrained ligand flexibility and partial flexibility of the binding pocket thus affording a more realistic environment for ligand-receptor associations.

As the tool does not have the provision for the preparation of proteins or ligands, other software programs (GLIDE/LigandFit) can be employed for the preparation of proteins and ligands for docking run. Taking the prepared protein and ligand, GOLD docking calculations were performed using default standard set of parameters. For each of the 10 independent GA runs, a maximum number of 100 GA operations were performed. The standard set parameters were used in all the calculations. Default operator weights were used for crossover, mutation, and migration of 95, 95, and 10, respectively. Default cutoff values of 2.5 Å (for hydrogen bonds) and 4.0 Å (for vdW) were employed. Pop. Size = 100; max ops = 100,000; niche size = 2 were also employed. To further speed up the calculation, the GA docking was terminated when the top three solutions were within 1.5 Å RMSD of each other. GOLD scores each binding mode using a fitness function that accounts for the steric and electrostatic complementarities between the ligand and receptor. The GOLD scoring function includes the terms for hydrogen-bonding, vdW and intramolecular energies. The first ranked solutions of the ligands were taken for further observation of binding orientation and H-Bond interactions.

Synthesis

Synthesis and characterization of the compounds were reported in our earlier paper [17] and the synthetic route has been presented in Scheme 1.

in vitro adenylyl cyclase activity assay

Due to the lack of a suitable radioligand the affinity of antagonists and the relative potency at A_{2B} AR were determined in adenylyl cyclase experiments. The procedure was carried out as described in the literature [27] with minor modifications. Membranes were incubated with about 150,000 cpm of [α-32P] ATP for 20 min in the incubation mixture as described [28] without EGTA and NaCl. For agonists the IC_{50}-values for the stimulation of adenylyl cyclase were calculated with the Hill equation. Hill coefficients in all experiments were near unity. IC_{50} values for concentration-dependent inhibition of NECA-stimulated adenylyl cyclase caused by antagonists were calculated accordingly.

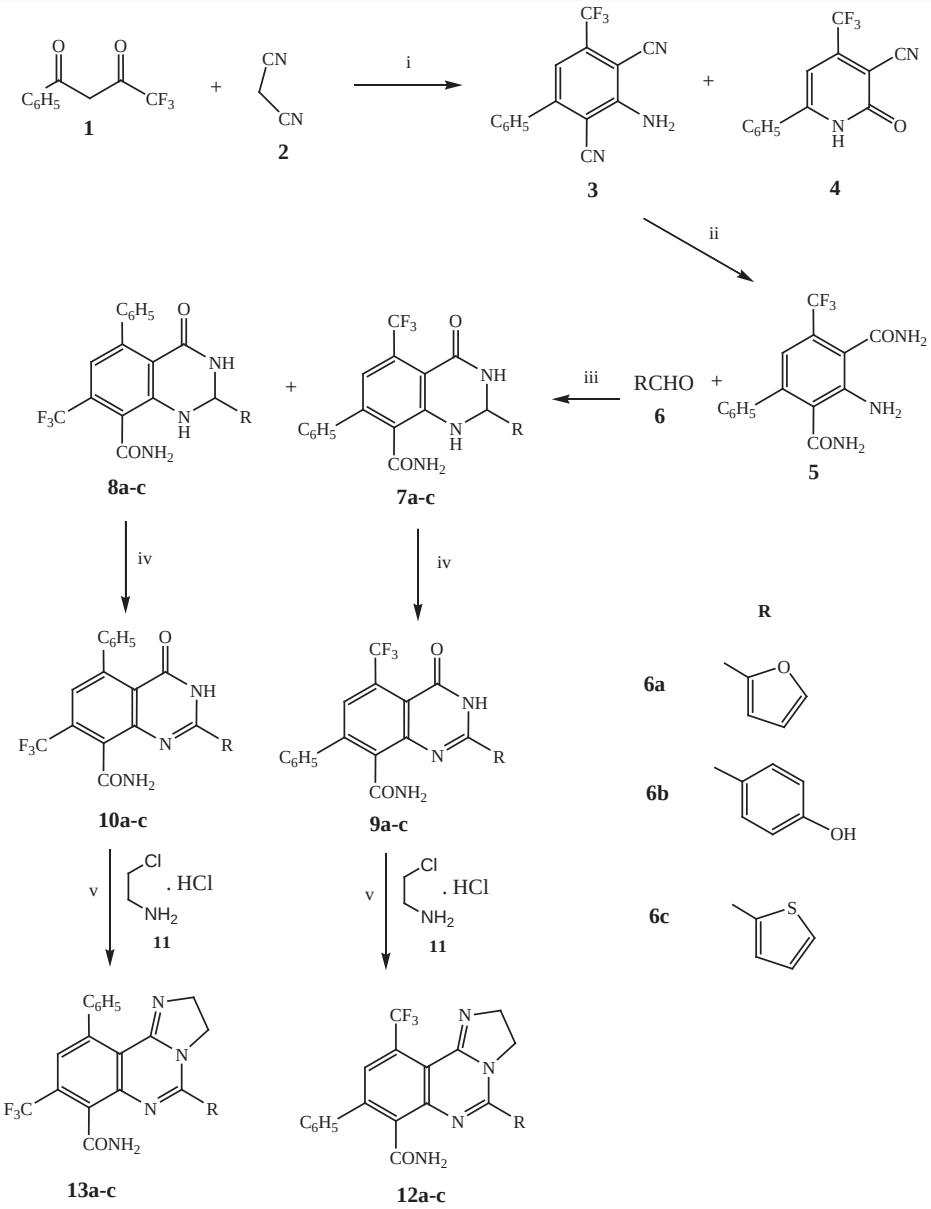

Scheme 1 Reagents and conditions: (i) methanol, reflux, 6 h; (ii) 20% KOH, reflux, 7 h; (iii) glacial acetic acid, r.t., 4 h; (iv) MnO2, dichloromethane, r.t., 2 h; (v) POCl3, reflux, 5 h.

RESULTS AND DISCUSSION

The percentage similarity of the virtual ligands to that of the reported compound (CMB 6446) was calculated which showed 45-71% similarity (virtual ligands). Code numbers in parentheses indicate the synthesized ligands Table 1, Figure 2,3.

MOLECULAR DOCKING ON A_{2B} AR MODEL

Validation of the binding-site of A_{2B} AR homology model

All the designed ligands were evaluated *in silico* (docking) to recognize their hypothetical binding mode using a molecular (homology) model of A_{2B} AR. To investigate and validate our data to scrutinize the ability of molecular docking, some of the reference ligands (xanthines and nonxanthines) (Figure 4) were docked onto the active-site of the receptor using the selected software tools.

Theophylline (a xanthine drug) was docked onto the binding-site of A_{2B} AR. The C-2 carbonyl oxygen of theophylline was found interacting with hydroxyl group of Ser92 by H-bond with a distance of 3.00 Å. Similarly, H-bond formation was observed with Asn282 (distance of 3 Å) and Trp247 (distance of 3.5 Å). These observations by different docking modules were well corroborated with the reported data [29]. The results of the molecular docking of the enprofylline, suggest that three amino acid residues (Ser92, Asn282 and Trp247) of the receptor directly interacted with the ligand. The Ser92 formed a H-bond with carbonyl group at 2nd position of the xanthine moiety

Table 1: Percentage similarity of the test series with CMB 6446.

Compd. Code	Substituent's			Similarity (%)
	R_1	R_2	R_3	
ARR/PL-1 (12a)	$-CF_3$	$-C_6H_5$	-furyl	47.90
ARR/PL-2 (13a)	$-C_6H_5$	$-CF_3$	-furyl	45.10
ARR/PL-3 (12b)	$-CF_3$	$-C_6H_5$	-4-hydroxyphenyl	71.68
ARR/PL-4 (13b)	$-C_6H_5$	$-CF_3$	-4-hydroxyphenyl	71.12
ARR/PL-5 (12c)	$-CF_3$	$-C_6H_5$	-thienyl	70.30
ARR/PL-6 (13c)	$-C_6H_5$	$-CF_3$	-thienyl	70.85
ARR/PL-7	$-CF_3$	$-C_6H_5$	-2-chlorofuryl	62.38
ARR/PL-8	$-C_6H_5$	$-CF_3$	-2-chlorofuryl	62.94
ARR/PL-9	$-CF_3$	$-C_6H_5$	-2-chloropyryl	69.10
ARR/PL-10	$-C_6H_5$	$-CF_3$	-2-chloropyryl	68.20
ARR/PL-11	$-CF_3$	$-C_6H_5$	-2-cyano,3,4-dimethylpyryl	62.46
ARR/PL-12	$-C_6H_5$	$-CF_3$	-2-cyano,3,4-dimethylpyryl	61.40
ARR/PL-13	$-CF_3$	$-C_6H_5$	-3-methylthienyl	67.30
ARR/PL-14	$-C_6H_5$	$-CF_3$	-3-methylthienyl	66.46

Table 2: The docking scores of the molecules with A_{2B} AR (homology model).

Compd. Code	DOCK Score (Accelrys)	GOLD Score (GOLD)	GScore (Glide)
ARR/PL-1 (12a)	83.25	20.5	-6.72
ARR/PL-2 (13a)	75.41	16.32	-4.36
ARR/PL-3 (12b)	86.61	25.55	-4.05
ARR/PL-4 (13b)	70.20	13.35	-3.82
ARR/PL-5 (12c)	57.27	21.50	-7.95
ARR/PL-6 (13c)	68.44	40.89	-7.90
ARR/PL-7	68.83	33.45	-6.33
ARR/PL-8	67.61	35.24	-5.88
ARR/PL-9	63.01	34.18	-6.7
ARR/PL-10	69.41	38.31	-7.93
ARR/PL-11	61.24	41.37	-6.36
ARR/PL-12	65.48	30.38	-6.85
ARR/PL-13	68.80	24.49	-7.51
ARR/PL-14	69.75	32.00	-6.84
CMB-6446 (Reference ligand)	81.21	27.12	-4.68

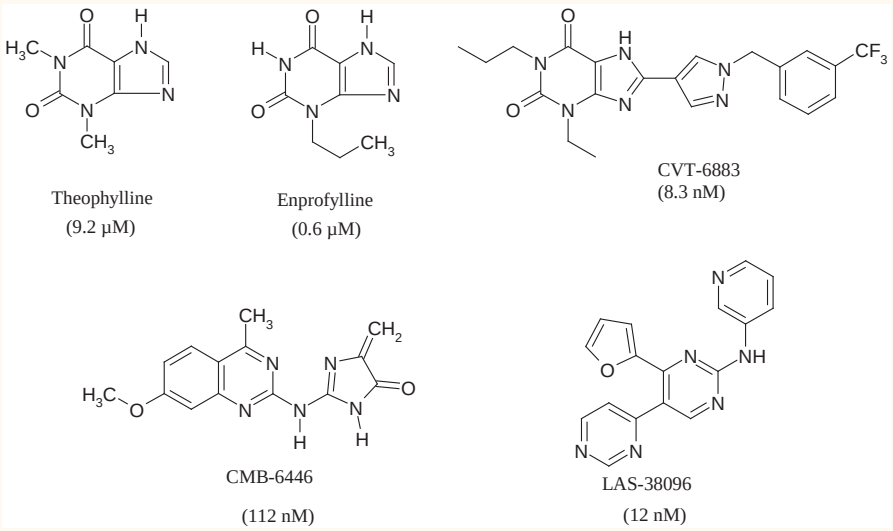

Figure 4 The A_{2B} AR antagonists used as reference standard and the values in parenthesis indicates their binding affinity towards A_{2B} AR.

(distance of 2.0578 Å), while Trp247 seems to be essential for binding because of a π-π interaction Figure 5a. These results are in agreement with the available data on the site-directed mutagenesis obtained for ARs. CVT-6883, a potent highly selective A_{2B} AR antagonist is located inside the hydrophobic pocket formed by Thr89, His251 and Val250. The *n*-propyl chain was located inside the two hydrophobic pockets formed by (i) Leu195, Met198 and Ala244 and (ii) Leu49, Asp53, Asn286 and Pro287. Additionally, Trp247 and Phe243 are involved in ligand binding *via* π-π interactions with the phenylxanthine moiety. Further the fluorine of trifluoromethyl group found interacting with Asn254 through H-bond at a distance of 2.1160 Å Figure 5b. Some of the nonxanthine derivatives (CMB-6446 and LAS-38096) were also docked onto the active-site of the receptor and interacted favourably with the amino acid residues. Methoxy oxygen of CMB-6446 (amino substituted quinazoline derivative) exhibited H-bond with Asn286 (distance of 2.2530 Å) and -NH at 2nd position interacted with Ser92 at a distance of 2.8606 Å Figure 5c. LAS-38096, a pyridinylbipyrimidine derivative, exhibited H-bond interaction between pyridinyl nitrogen and –NH of Asn282 (distance of 2.0043 Å). Furan oxygen showed H-bond interaction with Ser92 at a distance of 1.1029 Å. The orientation of pyrimidine ring in nonxanthine derivatives was found to be similar to that of pyrimidine ring of xanthine derivatives Figure 5d.

Docking of the test ligands on the validated active-site of A_{2B} AR

The fluorinated ligands were initially sketched and prepared as per the standard protocols of the used software packages. After the ligand preparation they were docked onto the active-site of the receptor model by employing three different docking modules. The docking scores of the ligands were represented in Table 2. The interaction between the designed ligands and active-site residues of A_{2B} AR were represented in Table 3.

Docking studies (GOLD) showed that all the ligands were docked well into the binding pocket of A_{2B} AR and engaged in favorable interactions with the active-site amino acid residues.

In ARR/PL-1, cyclic fused-ring system settled well in the binding pocket of the receptor model and trifluoromethyl group involved in H-bond with Trp247 (distance of 3.00 Å). Furan ring was surrounded by the residues of Ser165 and Asn163. Further a hydrophobic interaction was observed for carboxamido group with the residues of Ser279 and His280. In ARR/PL-2, carbonyl oxygen of carboxamido group showed a H-bond with amino nitrogen of Cys166 (distance of 1.83 Å) and a hydrophobic interaction with Ser165 (distance of 3.99 Å). The phenyl substituent at 8th position was located in a cavity surrounded by amino acid residues of Leu86, Val250, His251 and Asn254. The orientation of this ligand was found to be similar to that of its isomer (ARR/PL-1).

In ARR/PL-3, the carboxamido group of the ligand exhibited H-bond with hydroxyl group of Ser279. The van der Waals (vdW) interaction of carboxamido moiety with the residues of His280 and Val85 was also observed. The phenyl group was surrounded by Leu88 and Thr89. In ARR/PL-4, carboxamido group of the ligand exhibited H-bond with Cys166 and the phenyl ring was

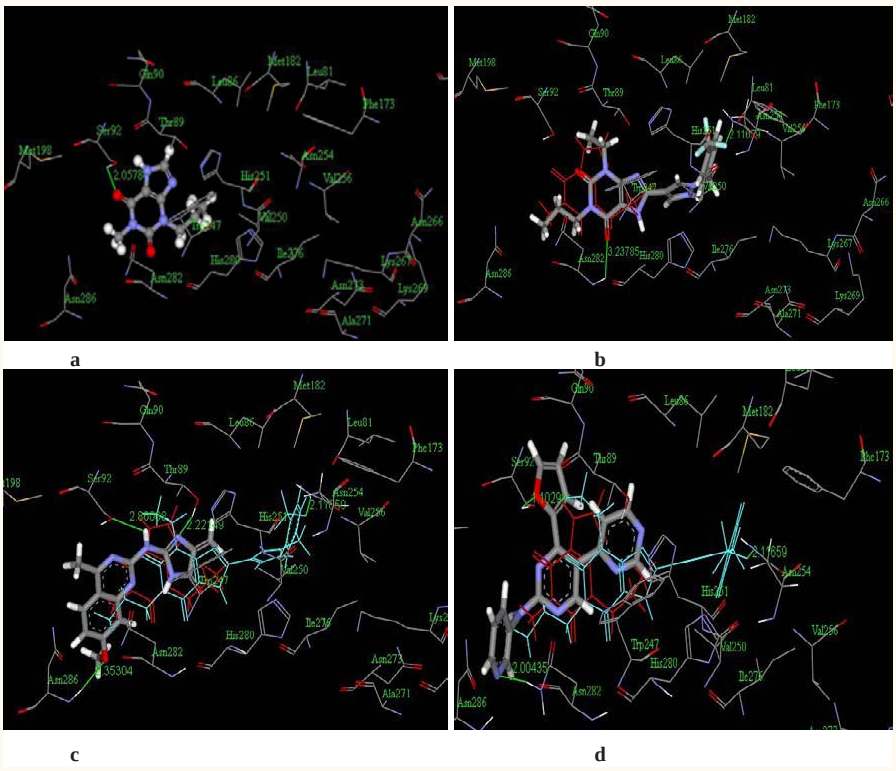

Figure 5 The A_{2B} AR antagonists used as reference standard and docked onto the active-site of A_{2B} AR a) Enprofylline; (b) CVT-6883 (c) CMB-6446; (d) LAS-38096 (Hydrogen atoms were hidden for clarity).

Table 3: The interacting ligands with active-site residues of A_{2B} AR.

S. No.	Compound	Interacting active-site residues (Type of interaction)
1	ARR/PL-1 (12a)	Trp247 (H-bond), His280 (van der Waals), Ser279 (van der Waals), Val250 (van der Waals), Asn282 (hydrophobic)
2	ARR/PL-2 (13a)	Cys166 (H-bond), Cys167 (van der Waals), Asn254 (van der Waals), Aln82 (van der Waals), Ieu276 (hydrophobic), Ser165 (hydrophobic)
3	ARR/PL-3 (12b)	Ser279 (H-bond), Val85 (van der Waals), Leu531 (van der Waals), Ser92 (hydrophobic)
4	ARR/PL-4 (13b)	Cys166 (H-bond), Val250 (van der Waals), Trp247 (π-π stacking), Cys78 (hydrophobic)
5	ARR/PL-5 (12c)	Ser279 (H-bond), His280 (van der Waals), Asn186 (van der Waals), Thr89 (hydrophobic), Ser92 (hydrophobic), Asn282 (hydrophobic)
6	ARR/PL-6 (13c)	Ser165 (H-bond), Cys167 (H-bond), Ser279 (hydrophobic), Asn282 (hydrophobic), Ile286 (hydrophobic), Ser279 (hydrophobic), Trp247 (hydrophobic)
7	ARR/PL-7	Ser279 (H-bond), Cys166 (van der Waals), Ser92 (hydrophobic), Val85 (hydrophobic), Trp247 (hydrophobic)
8	ARR/PL-8	Cys167 (H-bond), Leu86 (van der Waals), Ile286 (hydrophobic), Trp247 (hydrophobic)
9	ARR/PL-9	Cys167 (H-bond), Ile276 (H-bond), Leu86 (van der Waals), Val250 (hydrophobic), His251 (hydrophobic), Asn254 (hydrophobic),
10	ARR/PL-10	Ser165 (H-bond), Leu86 (van der Waals), Trp247 (hydrophobic), Ser92 (hydrophobic), Asn282 (hydrophobic)
11	ARR/PL-11	Ser279 (H-bond), Cys166 (van der Waals), Val250 (van der Waals), Trp247 (hydrophobic)
12	ARR/PL-12	Ser165 (H-bond), Trp247 (van der Waals), Cys166 (van der Waals), Ser279 (hydrophobic), Val85 (hydrophobic)
13	ARR/PL-13	Ser279 (H-bond), Ile276 (van der Waals), Asn254 (van der Waals), Thr89 (hydrophobic), Val85 (hydrophobic), Asn282 (hydrophobic)
14	ARR/PL-14	Cys166 (H-bond), Leu277 (van der Waals), Asn186 (van der Waals), Thr89 (hydrophobic), Asn286 (hydrophobic), Ser279 (hydrophobic)
15	CMB-6446	Asn282 (H-bond), Ser279 (H-bond), Thr89 (hydrophobic), and Trp247 (van der Waals)

Code numbers in parentheses indicate the synthesized ligands

surrounded by hydrophilic amino acid residues (Val250, Ile136 and Leu86). Further π-π stacking and hydrophobic interactions were observed with Trp247 and Cys78 respectively.

In ARR/PL-5, tricyclic fused-ring system settled well in the binding pocket of the receptor and -HN of carboxamido moiety interacted with hydroxyl group of Ser279 (distance of 1.92 Å). Further a strong hydrophobic interaction was also observed with the residues of Thr89, Ser92 and Asn282. The carboxamido group in ARR/PL-6 exhibited H-bond interaction with Ser165 (distance of 2.35 Å) and -F of CF_3 group with Cys167 (distance of 2.35 Å). Further a hydrophobic interaction was observed with the residues of Ser279, Asn282 and Trp247. Phenyl substituent at 10^{th} position was located in a hydrophobic cavity surrounded by amino acid residues of Val250, Thr89 and His251.

In ARR/PL-7, -HN of carboxamido group showed a H-bond with oxygen of Ser279 (distance of 2.22 Å). Phenyl substituent at 8^{th} position was surrounded by crucial amino acid residues (Asn282, Thr89, Cys246 and Trp247). The CF_3 group of the ligand was surrounded by the residues of Ser165, Cys166 and Trp247. In ARR/PL-8, -F of CF_3 group showed a H-bond with Cys166 (distance of 2.22 Å) and chloro substitution in pyrrole ring exhibited a strong hydrophobic interaction with Trp247.

In ARR/PL-9, -F of CF_3 group formed H-bond with Cys167 (distance of 1.82 Å) and -HN of carboxamido moiety showed H-bond with oxygen of Ile276 (distance of 2.15 Å). The substituted pyrrole ring exhibited hydrophobic interaction with the residues of Asn254, Asn186, His251 and Val250. In ARR/PL-10, the carboxamido group exhibited H-bond with Ser165 (distance of 2.00 Å). Further substituted pyrrole ring was surrounded by the residues of Asn186, Val250 and His251.

In ARR/PL-11, the carboxamido group exhibited a H-bond interaction with Ser279 (distance of 1.94 Å) and the phenyl ring was surrounded by the aromatic amino acid residues (Trp247 and Phe243). ARR/PL-12 had similar alignment and orientation as that of ARR/PL-11. Further a H-bond interaction was observed between the carboxamido group and Ser165 (distance of 2.02 Å).

In ARR/PL-13, -HN of carboxamido moiety exhibited a H-bond with Ser279 (distance of 2.23 Å). The thiophene moiety was surrounded by the residues of Leu277, Leu81 and Val85. The phenyl ring was surrounded by the residues of Trp247, Cys246, Phe243 and Asn282. In ARR/PL-14, -HN of carboxamido moiety showed a H-bond with Cys166 and the phenyl ring was surrounded by the residues of Asn254, His251, Val250, Thr89 and Trp247. Similar type of interactions was observed with other software tools (Glide and LigandFit). Various amino acid residues like Ser92, Trp247, Asn286, Leu49, Ser279, Cys167, Cys166, Cys246 and Thr89 were found to be crucial for ligand-receptor interactions.

Pharmacological studies

The synthesized compounds were evaluated for *in vitro* adenylyl cyclase activity against A_{2B} AR with an objective to obtain a fair correlation between *in silico* and *in vitro* observations. To our surprise, all the compounds showed moderate affinity (IC_{50} >30 μM) against A_{2B} AR in the assay of adenylyl cyclase activity. This moderate potency may be due to the presence of bulky aromatic substituents on fused-quinazoline moiety.

CONCLUSIONS

In this research work, we designed novel series of fluorinated heterofused quinazoline derivatives based on structural similarity and other related physico-chemical properties of potent quinazoline based A_{2B} AR antagonist. The designed ligands were considered further for molecular docking studies to ensure the efficiency of the ligands in binding to adenosine A_{2B} receptor. Among the three docking softwares, the comparative analyses on GOLD software indicated the better ligands interactions with crucial amino acid residues of the target protein. The selected ligands were synthesized, characterized spectroscopically and their preliminary anti-inflammatory evaluations were reported by our research group earlier. In this part of our investigations, we studied the implications of *in silico* tools in determining binding affinity of ligands towards hA_{2B} AR using *in vitro* studies. It has been concluded that the observed moderate binding efficiency of the ligands may be due to the steric factors exhibited by bulky substituents on the core nucleus. Further, efforts are being currently taken up to optimize the structure, synthesize a library of compounds, and *in vitro* pharmacological evaluation.

ACKNOWLEDGEMENTS

The authors thankfully acknowledge the Coordinator, Centre with Potential for Excellence in Biomedical Sciences (CPEBS) and Chairman, University Institute of Pharmaceutical Sciences (UIPS) Panjab University (PU), Chandigarh for providing facilities. Authors gratefully acknowledge Mrs. Lauren Thomas, CCDC, and Cambridge, UK for providing the GOLD software. One of the authors (CB) wishes to thank the University Grants Commission (UGC), New Delhi for providing PhD fellowship under UGC-RFSMS. This work was supported by AICTE, New Delhi Project Number: RPS- 8023/2006-07.

REFERENCES

1. Fredholm BB, IJzerman AP, Jacobson KA, Linden J, Muller CE. International Union of Basic and Clinical Pharmacology. LXXXI. Nomenclature and classification of adenosine receptors-an update. Pharmacol Rev. 2011; 63: 1-34.
2. Jacobson KA, Gao ZG. Adenosine receptors as therapeutic targets. Nat Rev Drug Discov. 2006; 5: 247-264.
3. Moro S, Gao ZG, Jacobson KA, Spalluto G. Progress in the pursuit of therapeutic adenosine receptor antagonists. Med Res Rev. 2006; 26: 131-159.
4. Müller CE, Scior T. Adenosine receptors and their modulators. Pharm Acta Helv. 1993; 68: 77-111.
5. Borea PA, Varani K, Vincenzi F, Baraldi PG, Tabrizi MA, Merighi S, et al. The A3 adenosine receptor: history and perspectives. Pharmacol Rev. 2015; 67: 74-102.
6. Aherne CM, Kewley EM, Eltzschig HK. The resurgence of A2B adenosine receptor signaling. Biochim Biophys Acta. 2011; 1808: 1329-1339.
7. Crespo A, El Maatougui A, Biagini P, Azuaje J, Coelho A, Brea J, et al. Discovery of 3,4-Dihydropyrimidin-2(1H)-ones As a Novel Class of Potent and Selective A2B Adenosine Receptor Antagonists. ACS Med Chem Lett. 2013; 4: 1031-1036.
8. Wei Q, Costanzi S, Balasubramanian R, Gao ZG, Jacobson KA. A2B adenosine receptor blockade inhibits growth of prostate cancer cells. Purinergic Signal. 2013; 9: 271-280.
9. Sepúlveda C, Palomo I, Fuentes E. Role of adenosine A2b receptor over expression in tumor progression. Life Sci. 2016; 166: 92-99.
10. Eisenstein A, Patterson S, Ravid K. The Many Faces of the A2b Adenosine Receptor in Cardiovascular and Metabolic Diseases. J Cell Physiol. 2015; 230: 2891-2897.
11. Müller CE, Jacobson KA. Recent developments in adenosine receptor ligands and their potential as novel drugs. Biochim Biophys Acta. 2011; 1808: 1290-1308.
12. Wang D, Gao F. Quinazoline derivatives: synthesis and bioactivities. Chem Cent J. 2013; 7: 95.
13. Khan I, Ibrar A, Abbas N, Saeed A. Recent advances in the structural library of functionalized quinazoline and quinazolinone scaffolds: Synthetic approaches and multifarious applications. Eur J Med Chem. 2014; 76: 193-244.
14. Webb TR, Lvovskiy D, Kim SA, Ji Xd, Melman N, Linden J, et al. Quinazolines as adenosine receptor antagonists: SAR and selectivity for A2B receptors. Bioorg Med Chem. 2003; 11: 77-85.
15. Gillis EP, Eastman KJ, Hill MD, Donnelly DJ, Meanwell NA. Applications of Fluorine in Medicinal Chemistry. J Med Chem. 2015; 58: 8315-8359.
16. Ferreira LG, Dos Santos RN, Oliva G, Andricopulo AD. Molecular docking and structure-based drug design strategies. Molecules. 2015; 20:13384-13421.
17. Balakumar C, Lamba P, Kishore DP, Narayana BL, Rao KV, Rajwinder K, et al. Synthesis, anti-inflammatory evaluation and docking studies of some new fluorinated fused quinazolines. Eur J Med Chem. 2010; 45: 4904-4913.
18. Chandrasekaran B, Deb PK, Rao VK, Bheemanapalli LN, Kaur R, Vishwakarma R, et al. Design, microwave-assisted synthesis and in silico docking studies of new 4H-pyrimido[2,1-b]benzothiazole-2-arylamino-3-cyano-4- ones as possible adenosine A2B receptor antagonists. Chem Incl Med Chem. 2012; 51: 1105-1113.
19. Banda V, Chandrasekaran B, Koese M, Vielmuth C, Mueller CE, Chavva K, et al. Synthesis of novel pyrido[3,2-e][1,2,4]triazolo[1,5-c] pyrimidine derivatives: potent and selective adenosine A3 receptor antagonists. Arch Pharm [Weinheim]. 2013; 346: 699-707.
20. Maggiora G, Vogt M, Stumpfe D, Bajorath J. Molecular similarity in medicinal chemistry. J Med Chem. 2014; 57: 3186-3204.
21. Venkatachalam CM, Jiang X, Oldfeild T, Waldman M. LigandFit: a novel method for the shape-directed rapid docking of ligands to protein active sites. J Mol Graph Model. 2003; 21: 289-307.
22. Glide Version 9.0. Schrodinger. New York. 2009.
23. GOLD 4.0.1. CCDC. CB21EZ, UK. 2008.
24. (a). Kiefer F, Arnold K, Kunzli M, Bordoli L, Schwede T. The SWISS-MODEL Repository and associated resources. Nucleic Acids Res. 2009; 37: 387-392;
25. (b) Arnold K, Bordoli L, Kopp J, Schwede T. The SWISS-MODEL Workspace: A web-based environment for protein structure homology modeling. Bioinformatics. 2006; 22: 195-201.
26. Klauda JB1, Brooks BR1. CHARMM Force Field Parameters for Nitroalkanes and Nitroarenes. J Chem Theory Comput. 2008; 4: 107-15.
27. Kaminski GA, Friesner RA, Rives JT, Jorgenson WL. Evaluation and reparameterization of the OPLS-AA force field for proteins via comparison with accurate quantum chemical calculations on peptides. J Phys Chem B. 2001; 105: 6474-6487.
28. Lohse MJ, Klotz K-N, Lindenborn FJ, Reddington M, Schwabe U, Olsson RA. 8-Cyclopentyl-1,3-dipropylxanthine (DPCPX)-a selective high

affinity antagonist radioligand for A1 adenosine receptors. Naunyn Schmiedebergs Arch Pharmacol. 1987; 336: 204-210.

29. Lean AD, Hancock AA, Lefkowitz RJ. Validation and statistical analysis of a computer modeling method for quantitative analysis of radioligand binding data for mixtures of pharmacological receptor subtypes. Mol Pharmacol. 1982; 21: 5-16.

30. Ivanov AA, Baskin I, Palyulin VA, Baraldi PG, Zefirov NS. Molecular modeling and molecular dynamics simulation of human A2B adenosine receptor: The study of the possible binding modes of A2B receptor antagonists. J Med Chem. 2005; 48: 6813-6820.

Cite this article

Chandrasekaran B, Deb PK, Akkinepalli RR (2017) Structure-based Design and Pharmacological Study of Fluorinated Fused Quinazolines as Adenosine A2B Receptor Antagonists. JSM Chem 5(2): 1041.